Effect of hydraulic hysteresis on dynamic response of unsaturated soils

B. Shahbodagh[a], N. Khalili, G. Alipour Esgandani

School of Civil and Environmental Engineering, The University of New South Wales, Sydney, NSW 2052, Australia

Abstract. Starting from the conservation laws, field equations governing the dynamic behaviour of unsaturated soils are presented. The coupling between solid and fluid phases is enforced according to the effective stress principle taking suction dependency and volume change of the effective stress parameters into account. The hydraulic hysteresis is accounted for through the effective stress parameter and the soil water characteristic curve. The spatial discretization of the governing equations is achieved using finite element method, whereas the time integration is conducted using the Newmark scheme. The numerical results are then presented, and the effect of hydraulic hysteresis on dynamic response of unsaturated soils is particularly emphasized.

1 Introduction

Despite the widespread distribution of unsaturated soils throughout the world, the development of constitutive and computational models for the dynamic behaviour of unsaturated soils has significantly lagged behind similar developments for dry and saturated soils. This has mainly been due to the inherent complexities associated with the dynamic behaviour of unsaturated soils, i.e. simultaneous flow of air and water through the porous materials, the presence of inertia forces in different phases, highly nonlinear deformation behaviour of the soil matrix, and complex interaction of fluid flow and deformation fields.

In recent years, several contributions have been made to dynamics of unsaturated soils. In the studies, two different approaches have generally been followed to enforce the coupling between solid and fluid phases. In the first approach, a single effective stress variable is used to describe the mechanical behaviour of unsaturated soils, e.g. see [1-7], while in the second approach two stress state variables, i.e. net stress and suction, are adopted to cast the constitutive relationships of the soil, e.g. see [8,9]. A major difficulty with the second approach is that it requires determination of two sets of material parameters, one for each of the stress state variables, which in fact may not be independent, and can lead to intractable stress strain relationships. In the effective stress based models developed for coupled dynamic analysis of unsaturated soils, the degree of saturation has mostly been used as the effective stress parameter. From experimental evidence, this parameter is strongly dependent on the soil structure and cannot be uniquely determined by the degree of saturation [10]. In addition, the effect of hydraulic hysteresis was ignored in the studies, which can significantly alter the response of unsaturated soils under dynamic loading conditions that can invariably involve complex cycles of strain-induced wetting and drying.

In this paper, a coupled flow-deformation model is presented for the dynamic/seismic analysis of unsaturated soils. The theoretical approach adopted is based on the model proposed by Khalili et al. [11], addressing the suction dependency and volume change of the effective stress parameter. The effect of hydraulic hysteresis on the effective stress parameter and soil water characteristic curve is accounted for using the model proposed by Khalili and Zargarbashi [12]. The spatial discretization of the governing equations is achieved using finite element method, whereas the time integration is conducted using the Newmark technique. The numerical results are then presented, demonstrating the performance of the proposed approach, and the effect of hydraulic hysteresis on static and dynamic response of unsaturated soils is particularly emphasized.

2 Basic Concepts

2.1. Effective Stress

The concept of effective stress plays a key role in quantitative assessment of response in saturated and unsaturated soils. In its most common form, the effective stress can be expressed as [13]

$$\sigma'_{ij} = \sigma_{net\ ij} - \chi s \delta_{ij} \tag{1}$$

where $\sigma_{net\ ij} = \sigma_{ij} + p_G \delta_{ij}$ is the net stress, $s = p_G - p_W$ is the matric suction, χ is the effective stress parameter, σ_{ij} is the total stress, p_W and p_G are the pore water and pore gas pressures, respectively, and δ_{ij} is the Kronecker

[a] Corresponding author: b.shahbodagh@unsw.edu.au

delta. The incremental form of the effective stress equation can be expressed as

$$\dot{\sigma}'_{ij} = \dot{\sigma}_{net\ ij} - \psi \dot{s} \delta_{ij} \tag{2}$$

where $\psi = \partial(\chi s)/\partial s$ is the incremental effective stress parameter, and superimposed dot denotes the time derivative with respect to the solid phase. Following the approach proposed by Khalili and Khabbaz [14] and Khalili et al. [15], the effective stress parameter is defined as

$$\chi = \begin{cases} 1 & \text{for } s \le s_e \\ (s/s_e)^{-\Omega} & \text{for } s > s_e \end{cases} \tag{3}$$

where Ω is a material parameter with the best fit value of 0.55, and s_e is the suction value marking the transition between saturated and unsaturated states. For wetting process, s_e is equal to the air expulsion value, s_{ex}, whereas for drying process, s_e is equal to the air entry value, s_{ae}. s_e is a priori a function of the specific volume or volume change of the solid skeleton. This leads to a shift to the right of the effective stress parameter curve and soil water characteristic curve with increasing density, see Figure 1.

Khalili and Zargarbashi [12] experimentally studied the effect of hydraulic hysteresis on the effective stress parameter, and proposed the following relation for suction reversals:

$$\chi = \begin{cases} \left(\frac{s_{rd}}{s_{ae}}\right)^{-\Omega} \left(\frac{s}{s_{rd}}\right)^{\zeta} & \text{for drying path reversal } \left(\frac{s_{ex}}{s_{ae}}\right)^{\frac{\Omega}{\Omega+\zeta}} s_{rd} \le s \le s_{rd} \\ \left(\frac{s_{rw}}{s_{ex}}\right)^{-\Omega} \left(\frac{s}{s_{rw}}\right)^{\zeta} & \text{for wetting path reversal } s_{rw} \le s \le \left(\frac{s_{ae}}{s_{ex}}\right)^{\frac{\Omega}{\Omega+\zeta}} s_{rw} \end{cases} \tag{4}$$

where ζ is the slope of the transition line between the main wetting and main drying paths in a $\ln\chi \sim \ln s$ plane, and s_{rw} and s_{rd} are the points of suction reversal on the main wetting and main drying paths, respectively.

2.2. Soil Water Characteristic Curve

Another important concept in the mechanics of unsaturated soils is the soil water characteristic curve (SWCC), which is used to determine the volumetric deformation of the water phase with respect to change in matric suction. In this formulation, the SWCC model proposed by Brooks and Corey [16], extended to include hydraulic hysteresis effect [11], is adopted as

$$S_{eff} = \begin{cases} 1 & \text{for } s \le s_e \\ (s_e/s)^{\lambda_p} & \text{for } s > s_e \end{cases} \tag{5}$$

$$S_{eff} = \begin{cases} \left(\frac{s_{ae}}{s_{rd}}\right)^{\lambda_p} \left(\frac{s_{rd}}{s}\right)^{\xi} & \text{for drying path reversal } \left(\frac{s_{ex}}{s_{ae}}\right)^{\frac{\lambda_p}{\lambda_p-\xi}} s_{rd} \le s \le s_{rd} \\ \left(\frac{s_{ex}}{s_{rw}}\right)^{\lambda_p} \left(\frac{s_{rw}}{s}\right)^{\xi} & \text{for wetting path reversal } s_{rw} \le s \le \left(\frac{s_{ae}}{s_{ex}}\right)^{\frac{\lambda_p}{\lambda_p-\xi}} s_{rw} \end{cases} \tag{6}$$

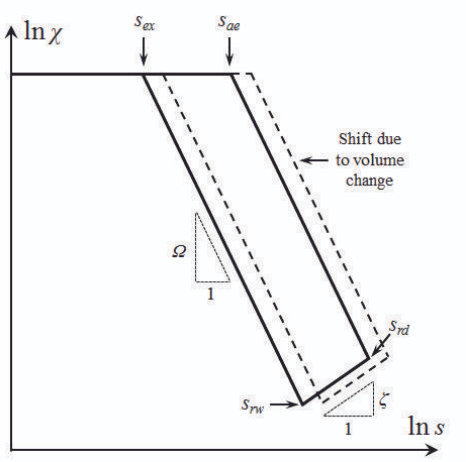

Figure 1. Evolution of the effective stress parameter χ with hydraulic hysteresis

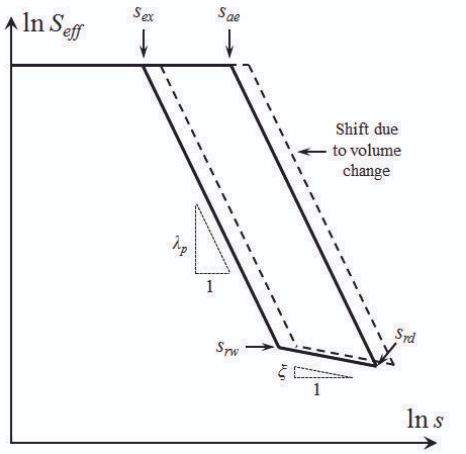

Figure 2. Soil water characteristic curve including hydraulic hysteresis

where λ_p is the pore size distribution index, $S_{eff} = (S_r - S_{res})/(1-S_{res})$ is the effective degree of saturation, and S_{res} is the residual degree of saturation, see Figure 2.

3 Governing Equations

3.1. Conservation of Mass

Unsaturated soils consist of three phases, i.e. solid (S), water (W), and gas (G), which within the context of theory of mixtures are assumed to be continuously distributed throughout representative elementary volume. By ignoring mass exchanges among the phases, the conservation of mass for each phase can be expressed by

$$\frac{d_\alpha}{dt}(n^\alpha \rho_\alpha) + n^\alpha \rho_\alpha v_{\alpha\, i,i} = 0 \qquad (\alpha = S, W, G) \tag{7}$$

where $v_{\alpha i}$ is the velocity vector of phase α, and $d_\alpha()/dt = \partial()/\partial t + ()_{,i} v_{\alpha i}$ is the material time derivative with respect to phase α. The material time derivative of volume fraction of fluid phases n^β $(\beta = W, G)$ with respect to the solid phase is obtained as

$$\frac{d_S n^\beta}{dt} = \frac{1}{V}\left(\frac{d_S V_\beta}{dt} - n^\beta \frac{d_S V}{dt}\right) = \frac{1}{V}\frac{d_S V_\beta}{dt} - n^\beta v_{S\,i,i} \tag{8}$$

in which V_α is the volume of constituent α, and V is the total volume. Assuming barotropic fluid, and substituting (8) into (7), we obtain

$$-\frac{1}{\rho_\beta}(\rho_\beta \dot{\omega}_{\beta i})_{,i} = n^\beta c_\beta \frac{d_S p_\beta}{dt} + \frac{1}{V}\frac{d_S V_\beta}{dt} \tag{9}$$

in which $\dot{\omega}_{\beta i} = n^\beta (v_{\beta i} - v_{S i})$ is the relative velocity of fluid phases with respect to the solid phase, and c_β is the compressibility coefficient for phase β. Invoking existence of elastic and plastic potentials, it can be shown that [11]

$$\frac{1}{V}\frac{d_S V_W}{dt} = \psi \dot{\varepsilon}_v + n\frac{\partial S_r}{\partial s}\dot{s} \tag{10}$$

$$\frac{1}{V}\frac{d_S V_G}{dt} = (1-\psi)\dot{\varepsilon}_v - n\frac{\partial S_r}{\partial s}\dot{s} \tag{11}$$

Substituting (10)-(11) into (9), the mass balance equations for the water and gas phases, respectively, become

$$-\frac{1}{\rho_W}(\rho_W \dot{\omega}_{W i})_{,i} = n^W c_W \frac{d_S p_W}{dt} + \psi \dot{\varepsilon}_v + n\frac{\partial S_r}{\partial s}\dot{s} \tag{12}$$

$$-\frac{1}{\rho_G}(\rho_G \dot{\omega}_{G i})_{,i} = n^G c_G \frac{d_S p_G}{dt} + (1-\psi)\dot{\varepsilon}_v - n\frac{\partial S_r}{\partial s}\dot{s} \tag{13}$$

3.2. Conservation of Momentum

The conservation of linear momentum of phase α gives

$$\sigma^\alpha_{ji,j} + \rho_\alpha n^\alpha b_i + \sum_{\gamma \neq \alpha} h_i^{\alpha\gamma} = \rho_\alpha n^\alpha a_{\alpha i} \tag{14}$$

where σ^α_{ij} is the partial Cauchy stress, $\gamma = S, W, G$, b_i is the body force per unit mass, $h_i^{\alpha\gamma} (= -h_i^{\gamma\alpha})$ is the interaction force per unit volume exerted by phase γ on phase α, and $a_{\alpha i}$ is the acceleration vector. Ignoring the relative accelerations between the phases and summing the conservation of momentum equations of the three phases yields

$$\sigma_{ji,j} + \rho b_i = \rho a_{Si} \tag{15}$$

where $\rho = \sum_\alpha \rho_\alpha n^\alpha$ is the density of the mixture, and ρ_α is the intrinsic density of phase α.

From the incorporation of the momentum balance equations into the mass balance equations, the continuity equations for the fluid phases become

$$\frac{1}{\rho_W}\left(\frac{k_W}{g}\left(p_{W,i} - \rho_W b_i + \rho_W a_{Si}\right)\right)_{,i} = n^W c_W \frac{d_S p_W}{dt} + \psi \dot{\varepsilon}_v + n\frac{\partial S_r}{\partial s}\dot{s} \tag{16}$$

$$\frac{1}{\rho_G}\left(\frac{k_G}{g}\left(p_{G,i} - \rho_G b_i + \rho_G a_{Si}\right)\right)_{,i} = n^G c_G \frac{d_S p_G}{dt} + (1-\psi)\dot{\varepsilon}_v - n\frac{\partial S_r}{\partial s}\dot{s} \tag{17}$$

3.3. Constitutive Equations

Constitutive relationships for volumetric deformations of fluid phases can be expressed as [11]

$$\frac{\dot{V}_W}{V} = \psi \dot{\varepsilon}_v + a_W \dot{s} \tag{18}$$

$$\frac{\dot{V}_G}{V} = (1-\psi)\dot{\varepsilon}_v + a_G \dot{s} \tag{19}$$

which relates the changes in pore fluid volumes to rates of suction and volumetric strain $\dot{\varepsilon}_v$. Due to highly nonlinear behaviour of soils, the stress-strain relationship of the soil skeleton is written in the incremental format as

$$\dot{\sigma}'_{ij} = C_{ijkl}\dot{\varepsilon}_{kl} \tag{20}$$

where C_{ijkl} is the constitutive tensor, and $\dot{\varepsilon}_{kl}$ is the soil skeleton strain tensor. The constitutive model adopted to express C_{ijkl} must be able to explain the deformation characteristics of the soil skeleton under cyclic loading conditions [11, 17-18].

4 Spatial and Temporal Discretization

For a quantitative solution, the weak forms of the equations of motion and flow continuity equations are obtained by applying the Galerkin method and spatially discretized using the finite element procedure. The primary unknown variables in the whole domain can be expressed in terms of the nodal values as

$$\{u\} = [N]\{u_N\} \quad , \quad p_\beta = \{N_h\}^T \{p_{\beta N}\} \tag{21}$$

where $[N]$ and $\{N_h\}$ represent the displacement shape functions for the solid phase, and the shape functions for the pore fluid pressures, respectively. The spatially discretized form of the governing partial differential equations can be written as

$$[M]\{\ddot{u}_N\} + [K]\{\Delta u_N\} - \chi[K_v]\{p_{WN}\} - (1-\chi)[K_v]\{p_{GN}\} = \{F\} - \{R\}_t \tag{22}$$

$$\rho_W \tilde{k}^W \left[K_v\right]^T \{\ddot{u}_N\} - \psi \left[K_v\right]^T \{\dot{u}_N\} - \tilde{k}^W [K_h]\{p_{WN}\} - c_{11}[K_n]\{\dot{p}_{WN}\} + c_{12}[K_n]\{\dot{p}_{GN}\} = -\tilde{k}^W \{q^W\} \quad (23)$$

$$\rho_G \tilde{k}^G \left[K_v\right]^T \{\ddot{u}_N\} - (1-\psi)\left[K_v\right]^T \{\dot{u}_N\} - \tilde{k}^G [K_h]\{p_{GN}\} - c_{22}[K_n]\{\dot{p}_{GN}\} + c_{12}[K_n]\{\dot{p}_{WN}\} = -\tilde{k}^G \{q^G\} \quad (24)$$

where $c_{11} = n^W c_W - n\partial S_r / \partial s$, $c_{22} = n^G c_G - n\partial S_r / \partial s$, $c_{12} = -n\partial S_r / \partial s$, $\tilde{k}^\beta = k^\beta / \rho_\beta g$, $\left[M\right]$ is the mass matrix, $\left[K\right]$ is the element stiffness matrix, $\left[K_v\right]$ is the coupling matrix, $[K_h]$ is the flow matrix, $[K_n]$ is the pore mass matrix, $\{q^W\}$ and $\{q^G\}$ are vectors of nodal fluxes of the water and gas flows, respectively, and $\{F\}$ and $\{R\}_t$ are the vectors of nodal forces. The definition of the finite element matrices can be found in [19]. The Newmark scheme is used for the time integration of the discretized governing equations, with the lowest allowable order for each primary variable. The unconditional stability of the Newmark scheme is achieved when $2\beta \geq \gamma \geq 0.5$ in which β and γ are the Newmark's parameters.

5 Numerical Examples

For the numerical analysis, a boundary value problem consisting of an unsaturated porous medium of 10 m height and 10 m width with an initial suction of 20 kPa is considered, see Figure 3. The mesh is composed of 400 mixed quadrilateral elements of dimensions 0.5 m×0.5 m. The upper boundary is drained and partially subjected to a load of width B=3.0 m with a uniform intensity f(τ), while the remaining boundaries are impervious. As the displacement boundary, the side boundaries are supported horizontally, and the bottom surface is vertically constrained. Table 1 shows the material parameters adopted for the analyses. The parameters for the fully saturated state are the same as those used by Simon et al. [20]. For the case with hydraulic hysteresis effect, the air entry and air expulsion values of s_{ae}=10 kPa, s_{ex}=5 kPa, along with ξ=0.04, and ζ=0.15 are used in the simulations, whereas for the case without hysteresis effect $s_{ae} = s_{ex}$ =10 kPa are adopted. The initial suction is assumed to be placed on the main drying path. In the case with hydraulic hysteresis, wetting and drying occurs along the scanning and main drying paths, respectively, whereas without hysteresis the wetting-drying cycles occur along the main drying path. The analyses are performed under a harmonic loading condition with angular frequency ω=62.83 rad/sec. A comparison of numerical results of the proposed hysteretic approach with those of the non-hysteretic approach is demonstrated in Figure 4 where $\hat{u}$ $\left(= uV_p\gamma_W s_{Ini} / (k_{Ws}\sigma_{\max} s_{ae})\right)$ is the normalized displacement and $\tau\left(= t\gamma_W / (\rho_{sat} k_{Ws})\right)$ is the normalized time. By taking the effect of hydraulic hysteresis into account, a deviation of the center line of the response from $\hat{u} = 0$ line is observed. Also, considering the hydraulic hysteresis in the analysis induces significantly larger variations in suction level during dynamic loadings.

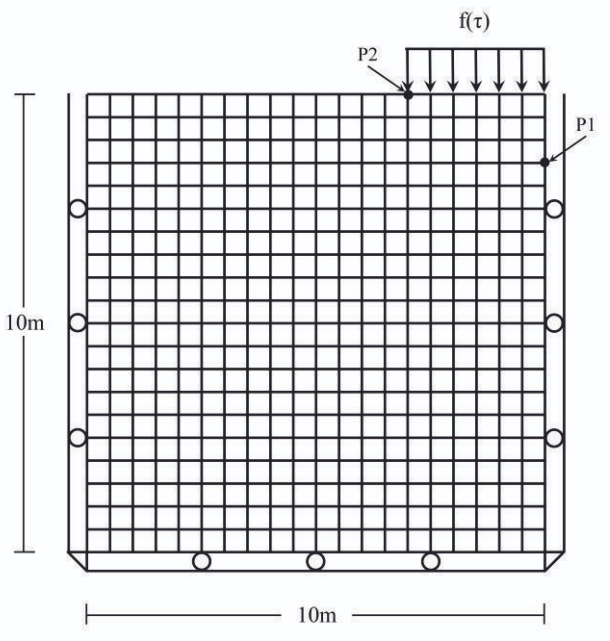

Figure 3. Finite element mesh and boundary conditions

6 Conclusions

A rigorous framework based on the theory of mixtures is presented for describing the dynamic behaviour of unsaturated soils. The coupling between solid and fluid phases is established through the effective stress principle taking suction dependency and volume change of the effective stress parameter into account. The hydraulic hysteresis is accounted for through the effective stress parameter and the soil water characteristic curve. The change in the degree of saturation due to a change in the volume of the pore at constant suction is also taken into account. The numerical results demonstrate that the hydraulic hysteresis markedly alter the response of unsaturated soils under dynamic loading condition.

Table 1. Material parameters considered for the analysis.

Initial void ratio	e_0	0.5
Lame's constant *(kPa)*	λ	833.3
Lame's constant *(kPa)*	μ	1250.0
Permeability of liquid at S_r=1 *(m/s)*	k_{Ws}	0.01425
Permeability of gas at S_r=0 *(m/s)*	k_{Gs}	0.05
Density of saturated mixture *(t/m^3)*	ρ_{sat}	1.8
Pore size distribution index	λ_p	0.15
Residual degree of saturation	S_{res}	0.2

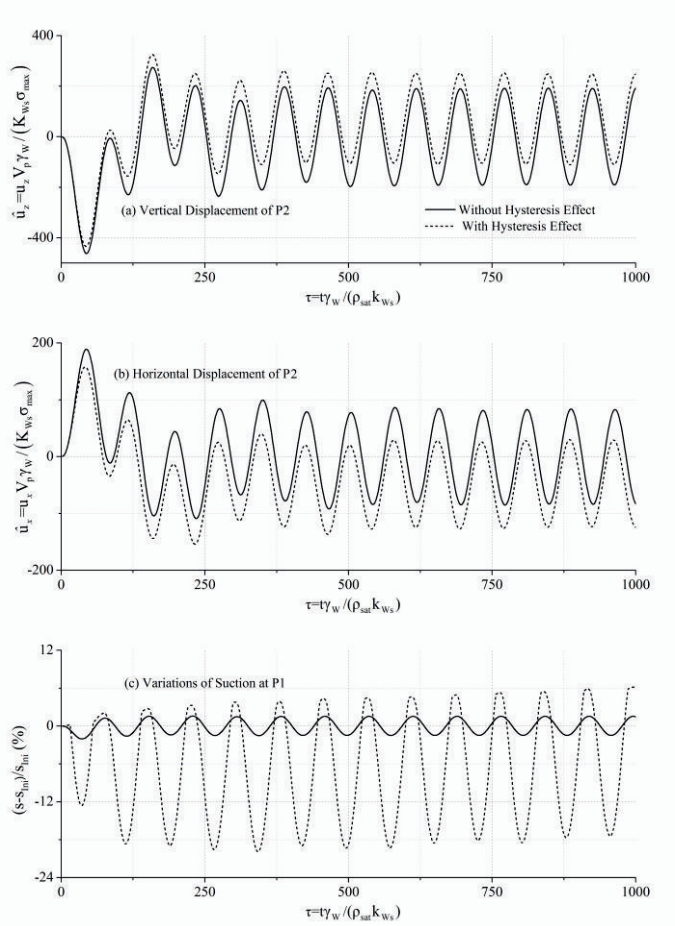

Figure 4. Effect of hydraulic hysteresis on dynamic response of the unsaturated porous medium

References

[1] Zienkiewicz OC, Xie YM, Schrefler BA, Ledesma A, Bičanič N. Static and dynamic behaviour of soils: a rational approach to quantitative solutions. II. Semi-saturated problems. *Proceedings of the Royal Society of London. Series A, Mathematical and Physical Sciences* 1990; **429**: 311-321.

[2] Meroi EA, Schrefler BA, Zienkiewicz OC. Large strain static and dynamic semisaturated soil behaviour. *International Journal for Numerical and Analytical Methods in Geomechanics* 1995; **19**: 81-106.

[3] Schrefler BA, Scotta R. A fully coupled dynamic model for two-phase fluid flow in deformable porous media. *Computer Methods in Applied Mechanics and Engineering* 2001; **190**: 3223–3246.

[4] Shahbodagh Khan B. Large deformation dynamic analysis method for partially saturated elasto-viscoplastic soils*, PhD dissertation*, Kyoto University, 2011.

[5] Uzuoka R, Borja RI. Dynamics of unsaturated poroelastic solids at finite strain. *International Journal for Numerical and Analytical Methods in Geomechanics* 2012; **36**: 1535-1573.

[6] B Shahbodagh, G Esgandani, N Khalili. Large deformation dynamic analysis of unsaturated soils. *The 6th International Conference on Unsaturated Soils, UNSAT 2014, Sydney*, 2014; 755 - 760.

[7] B Shahbodagh, N Khalili. A u-p formulation for fully coupled dynamic analysis of flow and deformation in unsaturated soils. *The 2nd Australasian Conference on Computational Mechanics, Brisbane,* 2015.

[8] Muraleetharan KK, Wei C. Dynamic behaviour of unsaturated porous media: governing equations using the Theory of Mixtures with Interfaces (TMI). *International Journal for Numerical and Analytical Methods in Geomechanics* 1999; **23**: 1579-1608.

[9] Ravichandran N, Muraleetharan KK. Dynamics of unsaturated soils using various finite element formulations. *International Journal for Numerical and Analytical Methods in Geomechanics* 2009; **33**: 611–631.

[10] Zerhouni MI. Application des réseaux de Petri continus à l'analyse dynamique des systèmes de production. *Thèse de Doctorat de l'INP Grenoble*, France; 1991.

[11] Khalili N, Habte MA, Zargarbashi S, A fully coupled flow deformation model for cyclic analysis of unsaturated soils including hydraulic and mechanical hystereses, *Computers and Geotechnics* 2008; **35**(6): 872-889.

[12] Khalili N, Zargarbashi S. Influence of hydraulic hysteresis on effective stress in unsaturated soils. *Geotechnique* 2010; **60**(9): 729-739.

[13] Bishop, A.W. 1959. The principle of effective stress. *Teknisk Ukeblad*;**106**(39): 859–863.

[14] Khalili N, and Khabbaz MH. A unique relationship for shear strength determination of unsaturated soils, *Geotechnique* 1998; **48**(5): 681-688.

[15] Khalili N., Geiser F, Blight G. Effective Stress in Unsaturated Soils: Review with New Evidence. *International Journal of Geomechanics* 2004; **4**(2): 115–126.

[16] Brooks RH, Corey AT. *Hydraulic properties of porous media: Hydrology Papers*. Colorado State University, Colorado, 1964.

[17] Oka F, Kimoto S. Computational modeling of multiphase geomaterials. CRC press, Taylor & Francis group, Boca Raton, London and New York, 2012.

[18] Kimoto S, Shahbodagh Khan B, Mirjalili M, Oka F. A cyclic elasto-viscoplastic constitutive model for clay considering the nonlinear kinematic hardening rules and the structural degradation, *International Journal of Geomechanics* 2013; **15**(5), A4014005.

[19] Shahbodagh Khan, B., Mirjalili, M., Kimoto, S. and Oka, F. 2013. Dynamic analysis of strain localization in water-saturated clay using a cyclic elasto-viscoplastic model, *International Journal for Numerical and Analytical Methods in Geomechanics* 2014; **38**(8), 771-793.

[20] Simon BR, Zienkiewicz OC, Paul DK. An analytical solution for the transient response of saturated porous elastic solids. *International Journal for Numerical and Analytical Methods in Geomechanics* 1984; **8**: 381-398.